Published in Applied Physics Letters, 103, issue 3, 031111-1/5, 2013
which should be used for any reference to this work

Wavelength tuning and thermal dynamics of continuous-wave mid-infrared distributed feedback quantum cascade lasers

Lionel Tombez,[1] Francesco Cappelli,[2] Stéphane Schilt,[1] Gianni Di Domenico,[1]
Saverio Bartalini,[2] and Daniel Hofstetter[1]
[1]*Laboratoire Temps-Fréquence, Institut de Physique, Université de Neuchâtel, Avenue de Bellevaux 51, CH-2000 Neuchâtel, Switzerland*
[2]*CNR-INO, Istituto Nazionale di Ottica and LENS, European Laboratory for Nonlinear Spectroscopy, Via Carrara 1, 50019 Sesto Fiorentino FI, Italy*

We report on the wavelength tuning dynamics in continuous-wave distributed feedback quantum cascade lasers (QCLs). The wavelength tuning response for direct current modulation of two mid-IR QCLs from different suppliers was measured from 10 Hz up to several MHz using ro-vibrational molecular resonances as frequency-to-intensity converters. Unlike the output intensity, which can be modulated up to several gigahertz, the frequency-modulation bandwidth was found to be on the order of 200 kHz, limited by the laser thermal dynamics. A non-negligible roll-off and a significant phase shift are observed above a few hundred hertz already and explained by a thermal model.

Since the first demonstration of quantum cascade lasers (QCLs) in 1994,[1] the number of promising application in the field of chemical sensing for biomedical and environmental sciences has been constantly rising during the last years. Indeed, thanks to the ability to tailor their emission wavelength and to target precisely selected ro-vibrational molecular transitions in the fingerprint region, QCLs were demonstrated to be very sensitive probes for a wide variety of molecules.[2] Single-frequency QCLs are generally required for trace gas sensing and a common approach is to use a distributed feedback (DFB) grating etched at the surface of the QCL active region in order to force laser operation at a precise wavelength.[3] Moreover, promising developments in the field of high-resolution spectroscopy can lead to the possibility of performing measurements with unprecedented precision, especially by linking spectrally narrow QCLs to optical frequency combs.[4,5] In order to push the limits of those high-resolution experiments, narrow-linewidth sources of coherent light which can be achieved by active stabilization of DFB-QCLs to optical references with high-bandwidth servo-loops are required.[6,7] For the most demanding applications in the field of high-resolution spectroscopy, frequency-noise analysis revealed that feedback loop bandwidths of several hundred of kHz are necessary for linewidth narrowing of DFB-QCLs.[7,8] While the picosecond carrier lifetime in QCLs allows a very fast modulation of the intensity above 10 GHz,[9,10] the modulation of the optical frequency—or wavelength—is limited by the thermal dynamics of the device. Indeed, unlike interband semiconductor laser diodes whose wavelength can be modulated at high speed through carrier density modulation,[11,12] the latter has no effect in QCLs because of the symmetric gain curve and associated independence of the refractive index at the gain peak (zero alpha parameter).[13] The wavelength tuning in DFB-QCLs is therefore mainly governed by the temperature dependence of the refractive index with a tuning rate of $1/\lambda\ d\lambda/dT \approx 7 \times 10^{-5}$ 1/K.[3] The ability to modulate the frequency of a QCL with the drive current at high speed is therefore limited by the thermal time constants in the structure, i.e., the time required for the temperature to follow the modulation of the dissipated electrical power. In Ref. 6, an important phase shift in the frequency-response was observed above a few tens of kHz already, which affects the feedback loop bandwidths and limits the ultimate achievable linewidth narrowing. Moreover, a rather low frequency-modulation bandwidth of 400 Hz was reported in Ref. 14. In this letter, we present in details the frequency modulation response of two different DFB-QCLs under direct current modulation in order to understand the dynamic behavior and bandwidth limitation that can occur in linewidth-narrowing experiments. The wavelength tuning dynamics is also of prime interest for the understanding of the underlying mechanism of frequency-noise generation and linewidth broadening in free-running QCLs.[15,16] Moreover, while the thermal resistance and the heat extraction of pulsed mid-IR[17–19] and THz QCLs[20] have been deeply investigated, our measurements allow us to discuss the dynamic of thermal effects in continuous-wave (CW) DFB-QCLs under direct current modulation. A simple thermal model allows us to fit the experimental results and extract the different thermal time constants involved in the system.

The frequency response of QCLs under direct current modulation was measured using a setup of single-pass direct absorption spectroscopy. The beam of the QCLs passes through a gas cell filled with carbon dioxide (CO_2) or carbon monoxide (CO) in a similar manner as in Refs. 7 and 8, respectively. The QCLs frequency was tuned to the flank of the respective molecular absorption line, which acts as a frequency-sensitive element. At this point, the frequency fluctuations of the laser are converted into intensity fluctuations that are detected with a photodiode. The conversion factor, or frequency discriminator, is given by the slope of the absorption line. Similar setups were used for frequency-noise characterization of free-running mid-IR[7,8] and THz[21] QCLs. For the measurements presented here, the current of the QCLs was modulated from 10 Hz up to several MHz and

TABLE I. QCLs main characteristics.

Device	Supplier	λ (μm)	Structure	i_{th} at 283 K (mA)	I_0 at 283 K (mA)	P_0 at 283 K (mW)
QCL1	Alpes Lasers	4.55	2.25 mm ridge epi-side up	300	350	5
QCL2	Hamamatsu	4.33	3 mm ridge epi-side down	660	710	5

the associated laser frequency modulation was measured in magnitude and phase using a lock-in amplifier. A small sinusoidal modulation on the order of 0.2 mA peak-to-peak was used in order to keep the laser frequency in the linear range of the molecular absorption line and to avoid any distortion of the output signal. It is important to note that the current driver and the photodiode have bandwidths of several MHz and more than 50 MHz, respectively, and therefore allow the measurement of the frequency modulation response of the QCLs up to several MHz without introducing any additional roll-off. Nevertheless, the laser intensity modulation response measured by detuning the laser out of the resonance was used to scale the magnitude and compensate for the slight phase shift introduced by the current driver at higher frequencies so that it reflects the dynamic response of the laser frequency only, as in Ref. 15. Two QCLs from different suppliers were characterized and compared. The first one is the same ridge waveguide DFB-QCL used in Ref. 7, emitting at 4.55 μm. The second one is a 4.33-μm distributed-feedback QCL from Hamamatsu Photonics.[8] These two devices are labeled QCL1 and QCL2, respectively, and their main characteristics are listed in Table I. QCL1 was mounted in a cryostat and its frequency-response was measured over a broad temperature range, from 283 K down to 85 K. QCL2 was mounted in a sealed package and its frequency response was measured at 283 K. The normalized frequency modulation response of QCL1 and QCL2 under direct current modulation is shown in Figs. 1(a) and 1(b), respectively. It is obtained from the ratio of the dynamic frequency-tuning coefficient to the static (DC) value. Both devices show a similar behavior. In the high-frequency region, a clear roll-off of -20 dB/decade and its associated phase shift are observed, in both cases beyond $\sim$200 kHz. In the low-frequency region, it is important to note that the frequency-response is not flat and differs from a first order low-pass filter. Indeed, a roll-off of a few dB/decade in the magnitude as well as a non-negligible phase shift is observed above a few hundred Hz already. At room-temperature, the frequency-modulation bandwidth of QCL2 is slightly higher than the one of QCL1. The frequency at which the phase shift reaches $-45°$ is $\sim$200 kHz for QCL1 and $\sim$300 kHz for QCL2, while the attenuation of the tuning coefficients is pretty strong and reaches a factor of 2 with respect to the DC value already at modulation frequencies lower than 100 kHz. It is important to note that one order of magnitude separates the $-45°$ and -3-dB frequencies, which supports the observation that the dynamic-response is not governed by a simple one-pole low-pass filter. The dynamic response of QCL1 was also measured over a large temperature range, from 283 K down to 85 K and is reported in Fig. 1(a) for these two extreme values. We observe that when the temperature is lowered, the modulation bandwidth increases and both the low-frequency roll-off and phase shift become smaller. The $-45°$ frequency increases from $\sim$200 kHz at room-temperature up to $\sim$400 kHz at 85 K. Moreover, the dynamic response at 85 K is qualitatively closer to a first order low-pass filter, with a weaker roll-off in the low-frequency range.

In order to have a deeper understanding of the observed dynamic responses and especially of the roll-off and phase shift at low frequency, a simple thermal model was used to fit the experimental data in magnitude and phase. On the other hand, a similar behavior has also been observed with conventional semiconductor laser diodes[11] for which an analytical model was derived;[22] we consider here the simple thermal response $R(f)$ consisting of three cascaded first-order low-pass filters (Eq. (1)) illustrated in Fig. 3(b). The fitted model is plotted along with the measured frequency modulation responses in Fig. 1 and shows a good agreement with

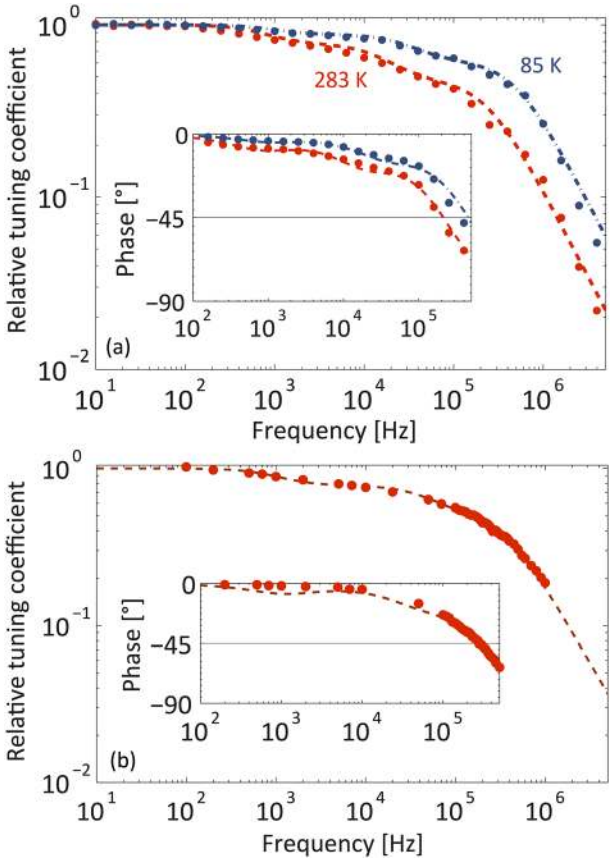

FIG. 1. Relative frequency-modulation of (a) QCL1 (at 85 K and 283 K) and (b) QCL2 (at 283 K) under direct current modulation ($I_{pp} = 0.2$ mA) and fitted model (dashed lines). The phase shift between frequency- and current-modulation is shown in the inset. In each case, the responses cannot be fitted with a one-pole low-pass filter but show a non-negligible roll-off and a significant phase shift above a few hundred hertz already. Then, a clear -20 dB/decade roll-off is observed above $\sim$200 kHz. The modulation bandwidth of QCL1 increases when the device is operated at 85 K. At room temperature, QCL2 shows a higher frequency-modulation bandwidth than QCL1.

TABLE II. Cut-off frequencies f_i and their relative contributions r_i (283 K).

Device	f_1 (kHz)	r_1	f_2 (kHz)	r_2	f_3 (Hz)	r_3
QCL1	200	0.46	16	0.31	550	0.23
QCL2	353	0.49	46	0.29	900	0.22

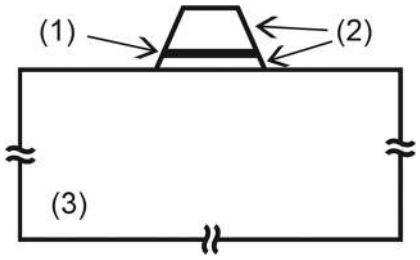

FIG. 2. Simplified diagram of the QCL cross-section. (1) Active core, (2) cladding, (3) substrate.

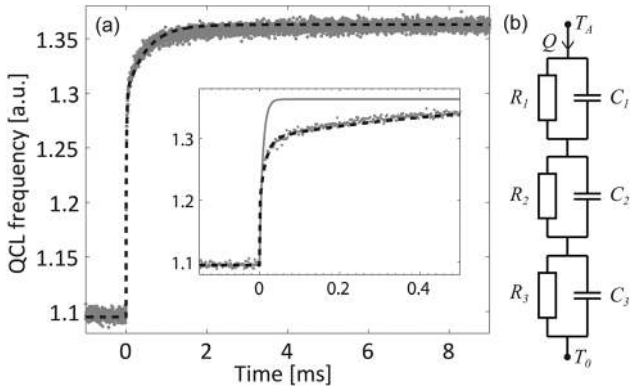

FIG. 3. (a) Experimental (grey points) and modeled (dashed line) time evolution of the QCL optical frequency when a current step is applied. Inset: zoom over the first 500 μs which shows a significant deviation from a simple 8-μs time constant exponential growth (solid line). After a fast heating of the active region and cladding during the first microseconds, it takes then several hundred of microseconds to reach the final temperature. (b) Thermal model used to fit the experimental data, where T_A is the average temperature of the active region, T_0 is the heat-sink temperature, Q is the heat flux, R_i is the thermal resistances, and C_i is the thermal capacitances.

both magnitude and phase experimental data. Assuming that the output frequency of the laser is a direct image of the average temperature in the active region and that the current modulation induces a proportional variation of the electrical power dissipated in the device, the frequency tuning response reflects therefore also the laser thermal response. The model parameters allow us to identify different thermal time constants in the system and their relative contributions r_i (Eq. (2)). It turns out that three different characteristic frequencies (f_1, f_2, f_3) are identified and reported with their respective normalized weights (r_1, r_2, r_3) in Table II for QCL1 and QCL2 at 283 K. These three characteristic frequencies are higher in QCL2, which is in agreement with the higher global modulation bandwidth observed in this device. Moreover, these experimental thermal time constants are on the same order of magnitude as the experimental values reported for a THz QCL[20] and simulation results obtained for pulsed QCLs.[19] The highest cut-off frequency, on the order of $f_1 = \sim 200$ kHz (corresponding to a time constant $\tau_1 = 1/2\pi f_1$ shorter than 1 μs), reflects the heat dissipation in the small volume of the active region itself, along the planes of the heterostructure. The second characteristic frequency $f_2 = \sim 20$ kHz likely corresponds to the heating due to heat extraction perpendicular to the planes of the heterostructure and through the waveguide layers. Indeed, the lower cross-plane thermal conductivity compared to the in-plane value,[17] the additional thermal resistivity of the cladding layers, and the larger associated volume contributes to this second longer thermal time constant. Finally, a third characteristic frequency f_3 lying below 1 kHz is attributed to the heat extraction through the substrate and the soldering which represent a relatively high thermal inertia compared to the waveguide and active region. These three distinct regions are illustrated in the simplified QCL cross section in Fig. 2. Fig. 3(a) shows the measured time evolution of the QCL optical frequency when a step of current is applied to the laser. It illustrates the deviation from a single exponential response. Indeed, the heating of the active region itself ($\tau_1 = 1$ μs, which cannot be resolved in the plot) and of the waveguide ($\tau_2 = 8$ μs) is pretty fast, it then takes more time ($\tau_3 = 400$ μs) to reach the final temperature because of the relatively high thermal inertia of the substrate and possibly of the soldering. The step response calculated from the thermal model is also plotted in Fig. 3(a) and shows a good agreement with the experimental data. From the experimental frequency-modulation response measured at different temperatures for QCL1, the different characteristic frequencies f_1, f_2, and f_3 were extracted and are plotted in Fig. 4 as a function of the laser heat-sink temperature. We observe that all these thermal cut-off frequencies increase when the device is cooled down over the considered temperature range, e.g., from 200 kHz at 283 K up to 500 kHz at 85 K for f_1. This is qualitatively in agreement with the fact that both the thermal resistivity and the specific heat of the semiconductor compounds of the QCL structure are monotonously decreasing with decreasing temperature in the considered range,[17,23] leading to higher thermal cut-off frequencies. From the parameters R_1, R_2, and R_3 determined from the fit, we also extracted the relative contribution r_i (Eq. (2)) of the thermal resistance of each part of the QCL structure to the total thermal resistance (Fig. 5). The contribution of the thermal resistance R_1 of the active core to the total thermal resistance is clearly dominant all over the temperature range.

$$R(f) = \frac{\Delta T}{\Delta P}(f) = \frac{R_1}{1+j\frac{f}{f_1}} + \frac{R_2}{1+j\frac{f}{f_2}} + \frac{R_3}{1+j\frac{f}{f_3}} \quad \text{with}$$

$$f_i = \frac{1}{2\pi R_i C_i}, \tag{1}$$

$$r_i = \frac{R_i}{R_1 + R_2 + R_3}. \tag{2}$$

Whereas, it amounts to 45% at room-temperature, the contribution of R_1 reaches almost 70% of the total thermal resistance at low temperature and explains the smaller roll-off observed in the low-frequency range at 85 K (Fig. 1). This behavior is attributed to the fact that the thermal

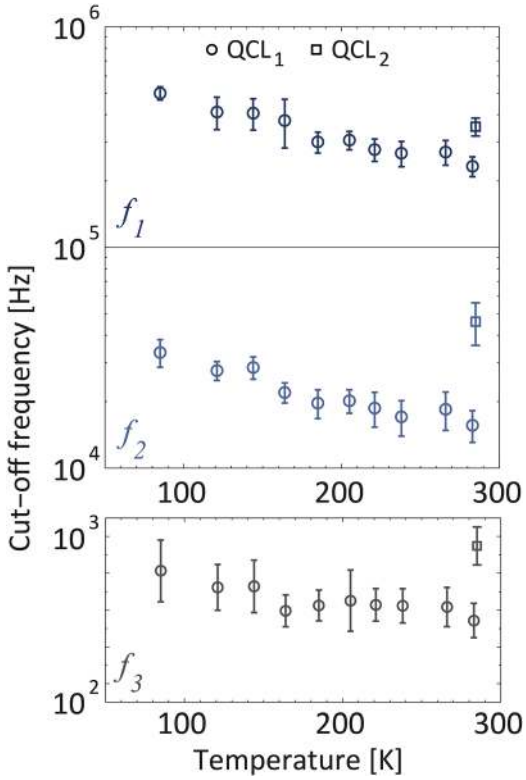

FIG. 4. Temperature dependence of the cut-off frequencies f_1, f_2, and f_3 extracted from the fit of the thermal model. All cut-off frequencies decrease with temperature. From 500 kHz at 85 K, f_1 decreases down to 200 kHz at room-temperature. QCL2 was found to benefit from higher cut-off frequencies, which is attributed to the junction-down mounting and associated lower thermal resistance.

resistivity of bulk InP decreases at a faster rate than the thermal resistivity of the heterostructure when the temperature is lowered.[17,24] The contribution of the thermal resistance of the substrate to the total thermal resistance becomes therefore weaker at low temperature, which increases the weight

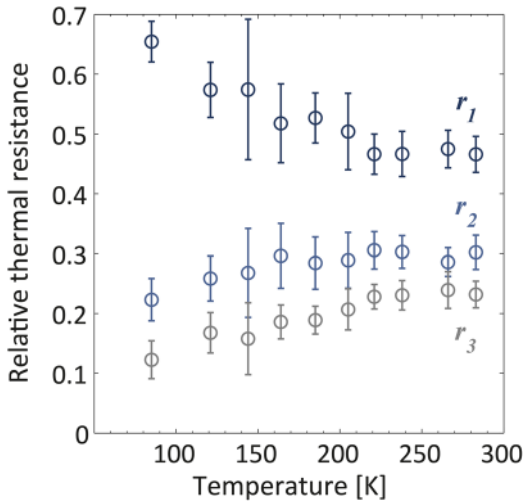

FIG. 5. Relative contributions r_1, r_2, r_3 of the model thermal resistances to the total thermal resistance (Eq. (2)). The contribution of the active region r_1 is dominant all over the temperature range and even increases when the temperature is lowered. At 85 K, it accounts for almost 70% of the total thermal resistance and explains the lower roll-off of the dynamic tuning coefficient of QCL1 observed in the intermediate frequency range at low temperature compared to room temperature.

of the fastest process (active region) in the global thermal behavior. This observation is in agreement with the dynamic response of the cryogenic QCL of Ref. 15 which was reported to behave like a one-pole low-pass filter. Finally, although the general behavior of QCL1 and QCL2 is very similar, it is important to note that the higher cut-off frequencies measured with QCL2 are very likely due to the junction-down mounting of this laser, which reduces the thermal resistance and therefore the thermal time constants. Device mounting might therefore be critical for applications requiring high frequency-modulation bandwidth and could be an important limiting factor for efficient linewidth narrowing. Although it is out of the scope of this letter, it is also worth mentioning that the model and method presented here could be useful for the determination of the thermal physical parameters of the QCL. Whereas we focused here on the dynamic behavior and fitted QCL relative frequency-responses, the use of the absolute frequency-tuning coefficients would allow R_i and C_i values of the model to be retrieved and for instance the specific heat of QCL heterostructures to be assessed. Finally, our study raises the question of frequency-modulation of QCLs at higher frequency (>100 MHz),[25] when the thermal tuning becomes negligible and frequency-modulation due to plasma-effect could possibly occur.

To conclude, we have presented the frequency-modulation response of two CW mid-IR DFB-QCLs under direct current modulation. Although a frequency-modulation bandwidth on the order of a few hundreds of kHz was obtained, a non-negligible roll-off and a significant phase shift appear above a few hundred Hz already. This behavior was analyzed and linked to the thermal dynamics in the lasers.

The authors from the University of Neuchâtel would like to acknowledge the financial support from the Swiss National Science Foundation (SNSF) as well as Alpes Lasers SA for providing useful information about the laser. The authors from CNR-INO and LENS would like to acknowledge Professor M. Yamanishi and Dr. N. Akikusa from Hamamatsu Photonics K. K. for having provided the room-temperature DFB QCL and the details about its design.

[1]J. Faist, F. Capasso, D. L. Sivco, C. Sirtori, A. L. Hutchinson, and A. Y. Cho, "Quantum cascade laser," Science **264**(5158), 553–556 (1994).
[2]K. Namjou, S. Cai, E. A. Whittaker, J. Faist, C. Gmachl, F. Capasso, D. L. Sivco, and A. Y. Cho, "Sensitive absorption spectroscopy with a room-temperature distributed-feedback quantum-cascade laser," Opt. Lett. **23**(3), 219–221 (1998).
[3]T. Aellen, S. Blaser, M. Beck, D. Hofstetter, J. Faist, and E. Gini, "Continuous-wave distributed-feedback quantum-cascade lasers on a Peltier cooler," Appl. Phys. Lett. **83**, 1929 (2003).
[4]I. Galli, M. S. de Cumis, F. Cappelli, S. Bartalini, D. Mazzotti, S. Borri, A. Montori, N. Akikusa, M. Yamanishi, G. Giusfredi, P. Cancio, and P. De Natale, "Comb-assisted subkilohertz linewidth quantum cascade laser for high-precision mid-infrared spectroscopy," Appl. Phys. Lett. **102**, 121117 (2013).
[5]A. Castrillo, A. Gambetta, D. Gatti, G. Galzerano, P. Laporta, M. Marangoni, and L. Gianfrani, "Absolute molecular density determinations by direct referencing of a quantum cascade laser to an optical frequency comb," Appl. Phys. B **110**(2), 155–162 (2013).
[6]F. Cappelli, I. Galli, S. Borri, G. Giusfredi, P. Cancio, D. Mazzotti, A. Montori, N. Akikusa, M. Yamanishi, S. Bartalini, and P. De Natale, "Subkilohertz linewidth room-temperature mid-infrared quantum cascade

laser using a molecular sub-Doppler reference," Opt. Lett. **37**, 4811–4813 (2012).

[7]L. Tombez, J. Di Francesco, S. Schilt, G. Di Domenico, J. Faist, P. Thomann, and D. Hofstetter, "Frequency noise of free-running 4.6 μm distributed feedback quantum cascade lasers near room temperature," Opt. Lett. **36**, 3109–3111 (2011).

[8]S. Bartalini, S. Borri, I. Galli, G. Giusfredi, D. Mazzotti, T. Edamura, N. Akikusa, M. Yamanishi, and P. De Natale, "Measuring frequency noise and intrinsic linewidth of a room-temperature DFB quantum cascade laser," Opt. Express **19**, 17996–18003 (2011).

[9]R. Paiella, R. Martini, F. Capasso, C. Gmachl, H. Y. Hwang, D. L. Sivco, J. N. Baillargeon, A. Y. Cho, E. A. Whittaker, and H. C. Liu, "High-frequency modulation without the relaxation oscillation resonance in quantum cascade lasers," Appl. Phys. Lett. **79**, 2526 (2001).

[10]F. Capasso, R. Paiella, R. Martini, R. Colombelli, C. Gmachl, T. L. Myers, M. S. Taubman, R. M. Williams, C. G. Bethea, K. Unterrainer, H. Y. Hwang, D. L. Sivco, A. Y. Cho, A. M. Sergent, H. C. Liu, and E. A. Whittaker, "Quantum cascade lasers: Ultrahigh–speed operation, optical wireless communication, narrow linewidth, and far-infrared emission," IEEE J. Quantum Electron. **38**, 511–532 (2002).

[11]S. Kobayashi, Y. Yamamoto, M. Ito, and T. Kimura, "Direct frequency modulation in AlGaAs semiconductor lasers," IEEE J. Quantum Electron. **18**(4), 582–595 (1982).

[12]P. Vankwikelberge, F. Buytaert, A. Franchois, R. Baets, P. I. Kuindersma, and C. W. Fredriksz, "Analysis of the carrier-induced FM response of DFB lasers: Theoretical and experimental case studies," IEEE J. Quantum Electron. **25**(11), 2239–2254 (1989).

[13]T. Aellen, R. Maulini, R. Terazzi, N. Hoyler, M. Giovannini, J. Faist, S. Blaser, and L. Hvozdara, "Direct measurement of the linewidth enhancement factor by optical heterodyning of an amplitude-modulated quantum cascade laser," Appl. Phys. Lett. **89**, 091121 (2006).

[14]L. Tao, K. Sun, D. Miller, M. Khan, and M. Zondlo, "Current and frequency modulation characteristics for continuous-wave quantum cascade lasers at 9.06 μm," Opt. Lett. **37**, 1358–1360 (2012).

[15]S. Borri, S. Bartalini, P. C. Pastor, I. Galli, G. Giusfredi, D. Mazzotti, M. Yamanishi, and P. De Natale, "Frequency-noise dynamics of mid-infrared quantum cascade lasers," IEEE J. Quantum Electron. **47**(7), 984–988 (2011).

[16]L. Tombez, S. Schilt, J. Di Francesco, P. Thomann, and D. Hofstetter, "Temperature dependence of the frequency noise in a mid-IR DFB quantum cascade laser from cryogenic to room temperature," Opt. Express **20**, 6851–6859 (2012).

[17]A. Lops, V. Spagnolo, and G. Scamarcio, "Thermal modeling of GaInAs/AlInAs quantum cascade lasers," J. Appl. Phys. **100**, 043109 (2006).

[18]M. S. Vitiello, T. Gresch, A. Lops, V. Spagnolo, G. Scamarcio, N. Hoyler, and J. Faist, "Influence of InAs, AlAs δ layers on the optical, electronic, and thermal characteristics of strain-compensated GaInAs/AlInAs quantum-cascade lasers," Appl. Phys. Lett. **91**(16), 161111 (2007).

[19]C. A. Evans, V. D. Jovanovic, D. Indjin, Z. Ikonic, and P. Harrison, "Investigation of thermal effects in quantum-cascade lasers," IEEE J. Quantum Electron. **42**(9), 859–867 (2006).

[20]M. S. Vitiello, G. Scamarcio, and V. Spagnolo, "Time-resolved measurement of the local lattice temperature in terahertz quantum cascade lasers," Appl. Phys. Lett. **92**, 101116 (2008).

[21]M. S. Vitiello, L. Consolino, S. Bartalini, A. Taschin, A. Tredicucci, M. Inguscio, and P. De Natale, "Quantum-limited frequency fluctuations in a terahertz laser," Nature Photon. **6**, 525–528 (2012).

[22]J. Buus, M. C. Amann, and D. J. Blumenthal, *Tunable Laser Diodes and Related Optical Sources* (Wiley-Interscience, New York, 2005), pp. 79–106.

[23]S. Adachi, *Physical Properties of III–V Semiconductor Compounds: InP, InAs, GaAs, GaP, InGaAs, and InGaAsP* (Wiley, New York, 1992).

[24]S. T. Huxtable, A. Shakouri, C. LaBounty, X. Fan, P. Abraham, Y. J. Chiu, and A. Majumdar, "Thermal conductivity of indium phosphide-based superlattices," Microscale Thermophys. Eng. **4**(3), 197–203 (2000).

[25]S. Borri, S. Bartalini, P. De Natale, M. Inguscio, C. Gmachl, F. Capasso, D. L. Sivco, and A. Y. Cho, "Frequency modulation spectroscopy by means of quantum-cascade lasers," Appl. Phys. B **85**, 223–229 (2006).